Synthetic PET Imaging for Grasping:
From Primate Neurophysiology to Human Behavior

M. A. Arbib[1], A. H. Fagg[1,3], and S. T. Grafton[2,4]

USC Brain Project[1] and Departments of Neurology and Radiology[2]

University of Southern California

Los Angeles, California 90089-2520

[3]Present Address: Computer Science Department, University of Massachusetts, Amherst, MA

[4]Present Address: Dartmouth College, Hanover, NH

Keywords: PET, neural networks, grasping, computational model, parietal cortex, premotor cortex, affordances

Correspondence: Please address all inquiries to M. A. Arbib, USC Brain Project, University of Southern California, Los Angeles, CA 90089-2520, USA. Email: arbib@pollux.usc.edu.

Abstract

Synthetic PET Imaging is a technique for using computational models derived from primate neurophysiological data to predict and analyze the results of human PET studies. This technique makes use of the hypothesis that rCBF (regional cerebral blood flow) is correlated with the integrated synaptic activity in a localized brain region. In this paper, we describe the Synthetic PET imaging approach, and demonstrate how it is applied to the FARS model of parietal-premotor interactions underlying primate grasp control. The Synthetic PET measures are computed for a simulated conditional/non-conditional grasping experiment, and then compared to the results of a similar human PET study. We then show how the human PET results may be used to further constrain the computational model.

1. Synthetic PET Defined

In order to provide a causal account of brain function constrained by data from both primate neurophysiology and human brain imaging, Arbib, Bischoff, Fagg, & Grafton (1995) introduced a new computational technique, called *Synthetic PET imaging.* This technique uses neural models that are based on primate neurophysiology to predict and analyze results from PET (Positron Emission Tomography) brain imaging of cerebral blood flow or glucose metabolism taken during performance of a variety of human behaviors. The problem is to find an integrated measure of activity in each simulated neural group that provides a predictor for the PET-measured activation of the 3D volume to which the neurons in this group correspond. The key hypothesis is that PET metabolic imaging is correlated with the integrated synaptic activity in a brain region (Brownell, Budinger, Lauterbur, & McGeer, 1982), and thus reflects in part neural activity in regions *afferent* to the region studied, rather than intrinsic neural activity of the region alone. However, the method is general, and can potentially accommodate other hypotheses on single cell correlates of imaged activity, and can thus be applied to other imaging techniques, such as functional MRI, as they emerge (see Arbib et al., 2000 for further discussion). Thus, although the present study uses Synthetic PET, we emphasize that this is but one case of the broader potential for systems neuroscience of Synthetic Brain Imaging (SBI) in general.

In the rest of this section we briefly review the way in which we represent neural networks for computer simulation, and then provide the formal definition for Synthetic PET.

Modeling Neural Networks: Here, we adopt the *leaky integrator* model of the neuron, in which the internal state of the neuron is described by a single variable, the *membrane potential* m(t) at the spike initiation zone. The time evolution of m(t) is given by the differential equation:

$$\boldsymbol{t}\frac{d\,m(t)}{dt} = -m(t) + \sum_i w_i X_i(t) + h,$$

(1)

with resting level h, time constant τ, $X_i(t)$ the firing rate at the ith input, and w_i the corresponding synaptic weight. The present model defines the firing rate as a continuously varying measure of the

cell's activity. The *firing rate* is approximated by a sigmoid function of the membrane potential, $M(t) = \sigma(m(t))$ [1].

Many brain regions can be modeled as a set of two dimensional arrays of neurons, with one array for each anatomically or physiologically distinct cell type. Connections between these neural arrays are defined in terms of interconnection masks which describe the synaptic weights. E.g., the equations

τ_A = 10 ms, and

$S_A = C + W*B$

state that the membrane time constant for neural region A, τ_A, is 10 milliseconds, and that for each cell i,j in array A, the cell's input, $S_A(i,j)$, is the sum of the output of the i,j[th] cell in C, plus the sum of the outputs of the 9 cells in B centered at i,j times their corresponding weights in W. In other words,

$$S_A(i,j) = C(i,j) + \sum_{k,l=-1}^{1} W(k,l)B(i+k,j+l).$$

That is, the * operator in "W*B" indicates that mask W is spatially convolved with B.

Defining Synthetic PET: The issue now is how to map the activity simulated in neural network models of interacting brain regions based on say single-cell recordings in behaving monkeys into predictions of metabolic activity values to be recorded from corresponding regions of the human brain by imaging techniques such as positron emission tomography (PET). There are two problems: localization, and modeling activation.

i)   *Localization:* Each array in the neural network model represents a neural population in a region identified anatomically and physiologically in the monkey brain. A Synthetic PET comparison requires explicit hypotheses stating that each such region A is homologous to a region h(A) in the human brain such that - within the tasks under consideration - A and h(A) perform their tasks in the same way. In some cases, such homologies are well defined. In other cases, the existence or identity of such a homology is an open question. Thus, the comparison of a Synthetic PET study with the results of a human brain scan study will, inter alia, be a test of the hypothesis "h(A) in human is homologous to A in (a given species of) monkey", and comparison of synthetic and human studies may suggest a new homology to be tested in further studies.[2]

ii)   *Modeling activation:* PET typically measures regional cerebral blood flow (rCBF). Arbib, et al. (1995) hypothesize that the counts acquired in PET scans are correlated with local synaptic activity in a particular region (Brownell, et al., 1982; Fox & Raichle, 1985), and call this

---

[1] An appreciation of neural complexity is necessary for the computational neuroscientist wishing to determine how detailed the neural model needs to be when studying a specific system - see (Rall, 1995) and the section on "More Detailed Properties of Neurons" in (Arbib, 1995c), for further details.

[2] See Bota and Arbib (2001) for the prototype of a database equipped with an inference engine for evaluating putative homologies.

measure the "raw PET activity". However, PET studies typically do not report these values, but instead report the comparative values of this activity in a given region for two different tasks or behaviors.

We thus define our Synthetic PET computation in two stages:

a) Compute $rPET_A$, the *simulated value of raw PET activity*, for each region A of our network while it is used to simulate the monkey's neural activity in some given task.

b) Compare the activities computed for two different tasks. The result is a Synthetic PET comparison which presents our prediction of human brain activity as based on neural network modeling constrained by monkey neurophysiology and known functional neuroanatomy.

The *synthetic raw activity,* $rPET_A$, associated with a cell group A is defined as:

$$rPET_A = \int_{t_0}^{t_1} \sum_B w_{B \to A}(t)\ dt, \tag{2}$$

where A is the region of interest, the sum is over all regions B that project to the region of interest, $w_{B \to A}(t)$ is the synaptic activity (*firing rate* * $|synaptic\ strength|$) summed over all the synapses from region B to region A at time t, and the time interval from t_0 to t_1 corresponds to the duration of the scan (see Arbib, et al., 1995 for further discussion).

The comparative activity $PET_A(1/2)$ for task 1 over task 2 for each region A was given by Arbib et al. (1995) as:

$$PET_A(1/2) = \frac{rPET_A(1) - rPET_A(2)}{rPET_A(2)}, \tag{3a}$$

where $rPET_A(i)$ is the value of $rPET_A$ in condition i, to compare the change in PET_A from task 2 to task 1. In the present study we use a different measure, defining the *relative synaptic activity* for region A from task 1 to task 2 with $\max(rPET_A(1), rPET_A(2))$ replacing $rPET_A(2)$ in the denominator of equation 3a to yield

$$PET_A(1/2) = \frac{rPET_A(j)}{\max_{i \in \{1,2\}} (rPET_A(i))} \tag{3b}$$

This yields a more robust measure of relative synaptic activity.

We can display the values of the "Synthetic PET comparison" $PET_A(1/2)$ for each region A on a graph or in a table, or we may (see Arbib, et al., 1995) convert each A-value to a color scale, and display the colors on the region h(A) homologous to A on slices based on the Talairach Atlas (Talairach & Tournoux, 1988). The resulting images then predict the results of human PET studies. Note that we are plotting *synaptic* activity for each region A, not the neural activity of A. As a computational plus (going beyond the imaging technology), we may also collect the contributions of the excitatory and inhibitory synapses separately, based on evaluating the integral in Eq. 2 over one set of synapses or the other.

Using simulated PET, we can break apart different factors that contribute to the measure of synaptic activity so that they can be studied independently. This can allow a much more informed view of the actual PET data that are collected, possibly shedding light on apparent contradictions that arise from interpreting rCBF simply as cell activity.

2. A Model of Grasp Control

The cells of area F5 of the macaque inferior premotor cortex are often selective for the type of grasp made by the monkey (Rizzolatti, Camarda, Fogassi, Gentilucci, Luppino, & Matelli, 1988). Grasps observed during these experiments include precision pinches (using the tips of the index finger and thumb), lateral pinches (thumb against the side of the index finger), and power grasps (four fingers opposing the palm). In addition, the firing of these cells typically correlated with a particular phase of the ongoing movement. For a task in which the monkey was presented with an object, then grasped the object in response to a go signal, held the object, and finally released the object after a secondary go signal, the following phases were identified: preparatory (set), finger extension, finger flexion, holding, and release. F5 exchanges cortico-cortical connections with the anterior intra-parietal area of parietal cortex (AIP), whose cells demonstrate a variety of both visual- and grasp-related responses (Taira et al., 1990).

This section outlines the FARS (Fagg-Arbib-Rizzolatti-Sakata) model of the grasping process. It is implemented in terms of simplified, but biologically plausible neural networks. For details of the model, supporting monkey data, computational constraints, and a set of simulation results, see Fagg (1996) and Fagg & Arbib (1998). In the next section, we will extract measures of regional synaptic activity from the model, and then compare them to rCBF results in a human PET study.

The FARS model focuses on the roles of several intra-parietal areas (AIP, PIP, and VIP), inferior premotor cortex (F4 and F5), pre-SMA (F6), frontal cortex (area 46), F2 (dorsal premotor cortex), inferotemporal cortex (IT), the secondary somatosensory cortex (SII), and the basal ganglia (BG). However, in this paper we shall discuss only the contributions of AIP, F5, F6, F2, and the BG. The crucial aspects of the model (see Figure 1) are the following:

1. AIP serves the dual role of first computing a **set of affordances** for the object being attended (i.e., AIP highlights properties of the object relevant for manually interacting with it), and then maintaining an **active memory** of the selected affordance as the corresponding grasp is prepared and executed.

2. F5 integrates a variety of constraints to decide on the single grasp that is to be executed. These constraints include visual information (from the affordances extracted by AIP), task information (from F6), instruction stimuli (from F2), and a working memory (from area 46) of recently-executed grasps. We shall say more of F6 and F2 below; area 46 will not be considered further in
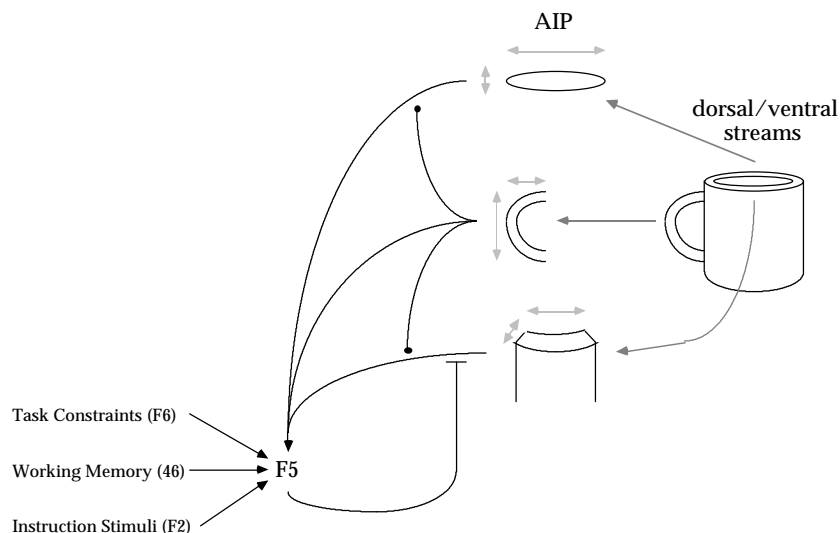
Figure 1: According to the FARS model, AIP uses visual input to extract affordances, which highlight the features of the object that are relevant to grasping it. F5 then applies various constraints to select a grasp for execution and to inform AIP of the status of its execution, thus updating AIP's active memory. The areas shown are AIP (anterior intraparietal cortex), area F5 (of the ventral premotor cortex), and regions providing supporting input to F5, namely F6 (pre-SMA), area 46 (dorsolateral prefrontal cortex), and F2 (dorsal premotor cortex).

the present paper. When the movement is triggered, F5 is responsible for the high-level execution and subsequent monitoring of the planned preshape and grasp.

Fagg & Arbib (1998) have offered both a computational analysis and an analysis of empirical data in support of the hypothesis that not only is F5 responsible for unfolding the grasp in time during the execution of the movement, but that F5 also sends recurrent connections back to AIP to update AIP's *active memory* for the grasp that is about to be executed or that is being executed by F5.

Figure 1 illustrates how the modeled AIP computes a set of affordances for a mug, and passes the corresponding set of grasps to F5. In general, a single object affords many possible grasps. As a function of the current context, F5 selects only one. This decision is then broadcast back to AIP, which shunts the other affordances, leaving only the affordance that corresponds to the selected grasp. During the execution of the grasp, the affordance represented by AIP forms the active memory which is continually updated by inputs from the active grasp program in F5. This process of separating out motor-related visual features may explain why cells in AIP reflect both object- and grasp-related activity patterns.

The *current context* used by F5 to select amongst available grasps may include task requirements, position of the object in space, and even obstacles. When the precise task is known ahead of time, it is assumed that a higher level planning region predisposes the selection of the correct grasp. In the FARS model, it is area F6 that performs this function. However, in this paper we emphasize a task in which the grasp is not known prior to presentation of the object, and is only determined by an arbitrary instruction stimulus made available during the course of the trial (e.g. an LED whose color indicates one of two

grasps). The dorsal premotor cortex (F2) is thought to be responsible for the association of arbitrary IS with the preparation of motor programs (Evarts, Shinoda, & Wise, 1984; Kurata & Wise, 1988; Wise & Mauritz, 1985). In a task in which a monkey must respond to the display of a pattern with a particular movement of a joystick, some neurons in F2 respond to the sensory-specific qualities of the input, but others specifically encode which task is to be executed on the basis of the instruction - they thus form *set cells* which encode the motor specification until the go signal is received (Fagg & Arbib, 1992; Mitz, Godshalk, & Wise, 1991).

We therefore implicate F2 as a key player in this grasp association task. What is particularly interesting about this type of conditional task, is that alone, neither the view of the object (with its multiple affordances), nor the instruction stimulus (IS) is enough to specify the grasp in its entirety: the visual input specifies the details of all the possible grasps; the IS specifies only the grasp mode—and not the specific parameters of the grasp (such as the aperture). F5 must combine these sources of information in order to determine the unique grasp that will be executed.

2.1 Population Coding of Grasp Type in AIP and F5

Figure 2 presents an outline of the neural regions involved in the FARS model of grasp production. The precision pinch and power grasp pools of AIP receive inputs from both the dorsal and ventral visual pathways (pathways not shown; more details may be found in Fagg, 1996 and Fagg & Arbib, 1998). The pools in F5 and AIP are connected through recurrent excitatory connections: affordances represented by populations of units in AIP excite corresponding grasp cells in F5; active F5 units, representing a selected grasp, in turn support the AIP units that extract the motorically-relevant features of the objects. In monkey, the number of neurons in F5 involved in the execution of the precision pinch is greater than the number observed for any other grasp (Rizzolatti, et al., 1988). The model reflects this distribution in the sizes of the precision and power pools in *both* F5 and AIP.

Each grasp pool within F5 is partitioned into overlapping subpopulations that encode both the phase of the grasp program, and the grasp parameters (e.g. the grasp aperture). Subpopulations within AIP capture the affordance parameters, such as object width. Cells within these subpopulations exchange excitatory connections with one another, supporting their mutual coactivation. Competition between opposing subpopulations is mediated via inhibitory interneurons (indicated by the connections in Figure 2 that are terminated with filled circles). F5 cells that are active for a given phase of movement recruit units in the primary motor cortex (F1) that move the fingers in a manner that is appropriate for that phase. In addition, units in the secondary somatosensory cortex (SII) are recruited by F5 cells as a way of monitoring the progress of the grasp as it is executed. The results of this monitoring are broadcast back to F5, which may in turn adjust the ongoing execution of the program.

When the model is presented with the conditional task described in the previous section, how is a unique grasp selected for execution? AIP first extracts the set of affordances that are relevant for the

presented object (say, a cylinder). These affordances, which also encode the diameter of the cylinder, activate the corresponding *motor set* cells in F5. However, because there are multiple active affordances, several competing subpopulations of F5 set cells achieve a moderate level of activation. This competition is resolved only when the IS is presented. This instruction signal, mapped to a grasp mode preference by the basal ganglia (connections not shown in the Figure), is hypothesized to arrive at F5 via F2. The signal increases the activation level of those F5 cells that correspond to the selected grasp, allowing them to win the competition over the other subpopulations.

Besides the processing of instruction stimuli, the basal ganglia play two additional roles in the model. A subset of BG units are dedicated to implementing the gating circuitry that controls the phasic behavior of cells within F5. This phasic activation, in turn, implements the set, preshape, enclose, hold, and release phases of the grasping motor program. This monitoring of the motor program takes place at a coarse level and is not specific to the type of grasp that is executed. In general, we imagine that F6 is responsible for configuring the gating circuitry so as to implement the appropriate sequence of movements. However, this knowledge is not explicitly represented in this implementation of the model. An additional set of BG cells is responsible for providing task specific biases for the grasp selection process. These cells also receive this bias information from area F6.
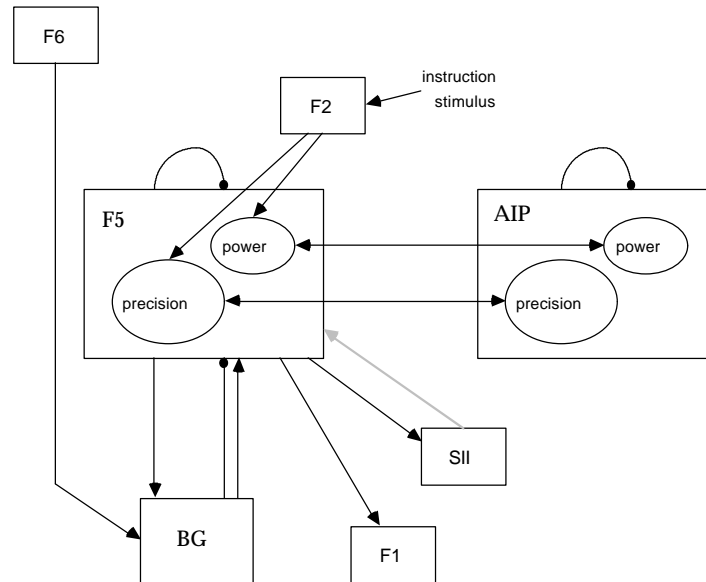
Figure 2: A schematic view of the model's architecture. Arrows indicate excitatory connections between regions; filled circles indicate inhibitory connections. The precision pinch and power grasp pools in F5 and AIP are connected through recurrent excitatory connections. The precision pinch pool contains more neurons than other grasps, which effects the Synthetic PET measure in these and downstream regions. F6 (pre-SMA) represents the high-level execution of the sequence, phase transitions dictated by the sequence are managed by the basal ganglia (BG). The dorsal premotor cortex (F2) biases the selection of grasp to execute as a function of the presented instruction stimulus.

2.2 Control of Sequential Behavior

The SMA has been implicated in the planning and execution of complex movements (Tanji & Keisetsu, 1994). In the FARS model, area F6 (pre-SMA) is responsible for representing the high-level sequence for performing the task (wait-grasp-hold-release). This region manages the phase-related activity in F5 and F4 (ventral premotor region involved in reaching movements) via pathways through the basal ganglia (see Figure 2).

F6 first prepares the ventral premotor regions for execution of the coming grasp by priming F4 and F5. This priming process allows set cells within F5 to become active in response to inputs from AIP. In response to the *go signal* given by the experimenter, F6 initiates execution of the program by priming movement-related cells in F5, and shunting set cells. Local excitatory and inhibitory interactions within F5 ensure that the selected grasp, as represented by F5 set cell activity at the time of the go signal, gives way to activation of the appropriate subpopulations of F5 movement (extension) cells.

Phase transitions in F5 from *extension* to *flexion*, and from *flexion* to *holding* are triggered by either an internal model of the hand state, or directly by sensory feedback from the hand (available from SII). Initiation of the *release phases* of movement is also managed by F6 in response to the second go signal.

3. Synthetic PET for Grasp Control

In what follows, we present the results of two different Synthetic PET experiments, which serve as predictions for what we expect when the experiments are performed in the human. In both experiments, the modeled subject is asked to grasp a single object using one of two grasps.

1. In the first experiment, we examine the effects of knowing which grasp to use prior to the onset of recording (non-conditional task), as compared with only being told which grasp to use after a delay period (conditional task). In the conditional task, an instruction stimulus in the form of a bi-colored LED informs the subject which grasp should be used.

2. The second experiment looks at the differences in rCBF between a "complex" grasp (precision pinch), and a "simple" grasp (power grasp).

For both experiments, we report the relative synaptic activity for each brain region and task. In addition, the comparative activity for each brain region is painted onto a three-dimensional model of a brain, which is derived from a Talairach-registered MRI image. Table 1 reports the location of each brain region and the experimental sources from which locations were derived. Regions on the surface of the model were painted if they fell within an ellipsoid surrounding the reported Talairach coordinate. The dimensions of the ellipsoids were scaled so as to bring the activation to the closest surface of the three-dimensional model.

Brain Region	Talairach Coordinates			Source	Experimental Context
	X	Y	Z		
F5	-64	4	24	Ehrsson et al., 2000 consistent with Buccino et al., 2001	Precision vs power grip Action observation
AIP	-40	-40	40	Binkofski et al., 2000 consistent with Buccino et al., 2001	Finger movement observation Action observation
F1 complex	-26	-24	38	Kinoshita et al., 1999	Precision grip for lifting
SII	-64	-20	24	Binkofski et al., 1999	Object manipulation
F2	-31.5	-6.1	54.2	Kurata et al., 2000	Conditional finger movement

Table 1: Talairach coordinates for modeled brain regions.

3.1 Comparison of Conditional and Non-Conditional Tasks

Figure 3A shows the relative synaptic activity measures for the conditional and non-conditional tasks (Experiment 1). Only regions in the model that demonstrate a change in synaptic activity from one task to the other are shown.
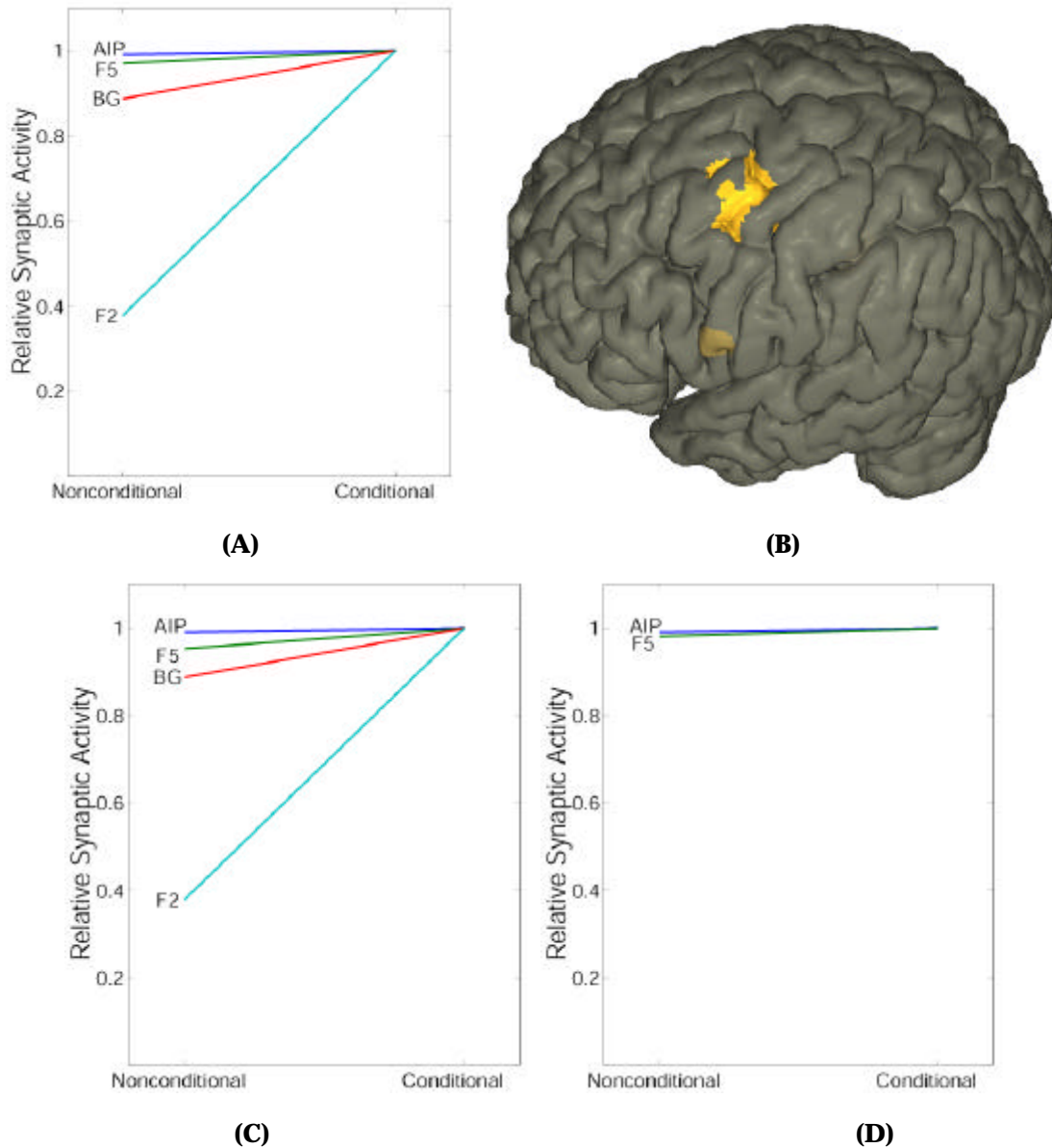
(A)

(B)

(C)

(D)

Figure 3: (A) Predictions of relative synaptic activity for the non-conditional and conditional tasks. Relative synaptic activity is defined as in Eq. 3b. A positive slope implies an increase in relative synaptic activity from the non-conditional to the conditional task. (B) The predicted PET image that highlights the conditional synaptic activity over non-conditional activity; the brightness of the gold color is proportional to $rPET_A(1/2)$. (C and D) Positive and negative synapse contributions to the synaptic activity measure for the same pair of tasks.

The most significant change predicted by the model is the level of activity exhibited by area F2 (dorsal premotor cortex). Its high level of activity in the conditional task is due to the fact that this region is only involved when the model must map an arbitrary stimulus to a motor program. In the non-conditional task, the region does not receive IS inputs, and thus its synaptic activity is dominated by the general background activity in the region. The additional IS inputs in the conditional task have a second-order effect on the network, as reflected in the small changes in synaptic activity in F5, BG, and AIP. The increased synaptic activity in F5 is due to the additional positive inputs from F2. These inputs also cause

an increase in the region's *activity level,* which is passed on through excitatory connections to both AIP and BG (recall Fig. 2).

It is important to note that synaptic activity does not have the same meaning as *neural activity*. This can be seen by examining the definition of $w_{B \rightarrow A}$(t) (see equation 2 of Section 1). The absolute value of the synaptic strength contributes positively to this measure—so increases in either positive *or* negative signals into a region will be reflected as an *increase* in synaptic activity. Neural activity, on the other hand, increases with excitatory input but decreases with inhibitory input. An important property of the Synthetic PET technique is that the positive and negative contributions to the Synthetic PET measure can be differentiated in the simulation. This information, combined with knowledge of the gross anatomy (especially the sign of connections between regions), can aid in inferring changes in neural activity across tasks.

Figures 3 C,D demonstrate the positive and negative contributions, respectively, to the overall PET measure in the conditional/non-conditional task comparison. Note that although the positive contributions to F5 and AIP essentially dominate the full PET measure, we also see small increases in the negative inputs into these regions. These inhibitory signals are due to negative inputs from local recurrent connections in the respective areas (in the case of F5, BG also contributes additional negative inputs). This serves as additional evidence that both F5 and AIP experience increases in their overall neural activity.

3.2 Comparison of Complex and Simple Grasps

As noted in Sec. 2.1, the model reflects the fact that the number of F5 neurons involved in the execution of the precision pinch is greater than those involved in the power grasp. We now show how this distribution is reflected in the Synthetic PET measures. The protocol used during Experiment 2 was the same as the non-conditional task described above.

Figure 4 illustrates a general increase in synaptic activity in many of the model's regions for the precision pinch over the power grasp. This effect is due to the larger number of participating units in F5 and AIP for the precision pinch case (see Figure 2). Not only is there a larger number of cells contributing to the rCBF measure, on average, but also each unit in the "precision pools" of AIP and F5 receives a greater number of positive inputs from other precision units.

Furthermore, despite the fact that the number of participating cells has only changed in F5 and AIP, we also observe an increase in synaptic activity in BG, F1, and SII. This is due to the fact that these regions receive input from a larger number of F5 neurons during the precision pinch task. Because these regions receive positive connections from F5 (Figure 2), this is an indication for a true increase in *cell activity* in F5 for the precision pinch case.
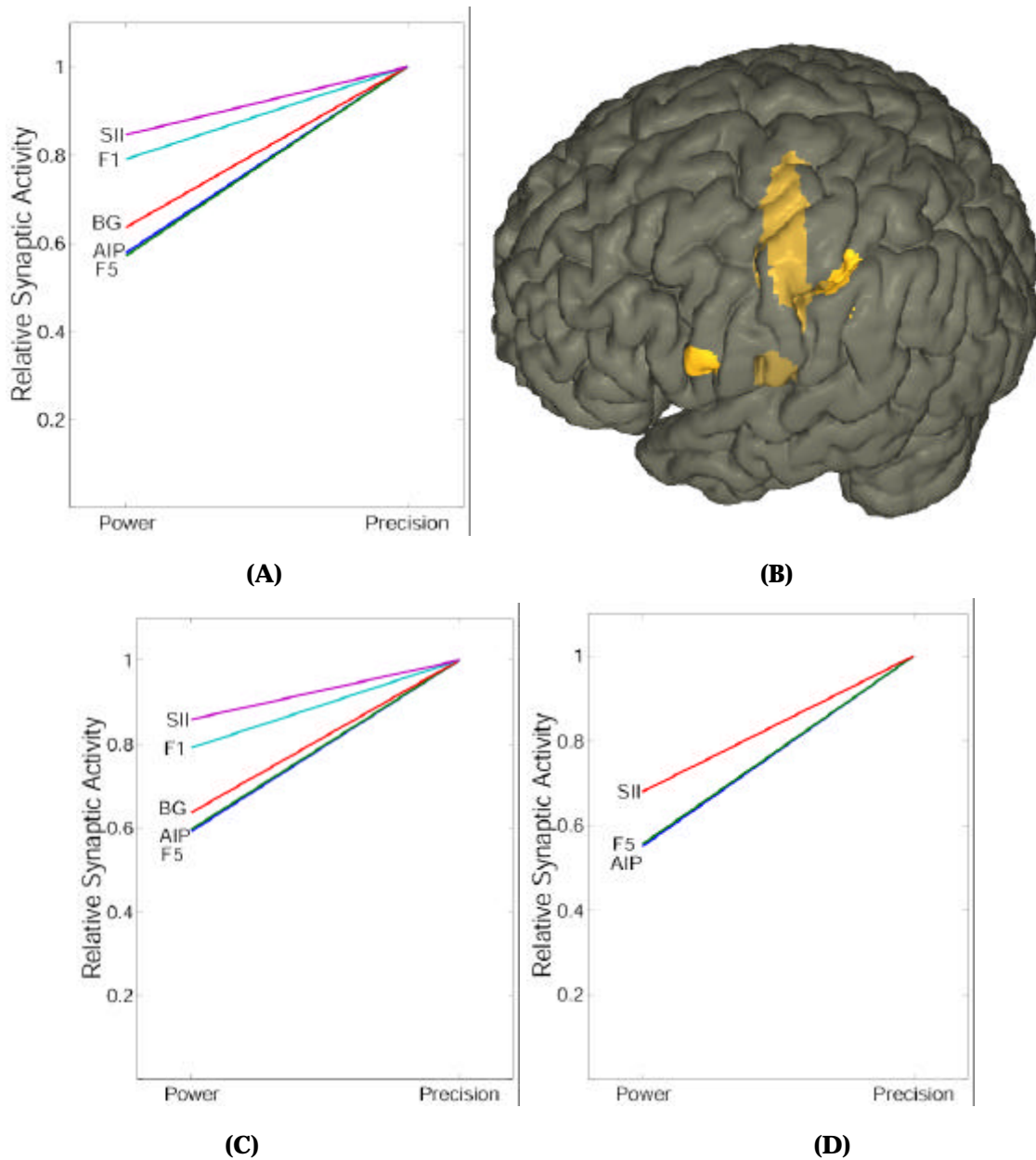
Figure 4: (A) Predictions of relative synaptic activity for the precision pinch and power grasp tasks. (B) Predicted PET image (precision versus power grasp). (C and D) Positive and negative synapse contributions to the synaptic activity measure the corresponding tasks.

4. Human Grasping Experiments

The Synthetic PET experiments described above raise some important questions about how instruction stimuli are mapped to arbitrary motor programs, and about the relative representation of different grasps. In this section, we summarize the results of a human PET experiment in which both of these questions were addressed (see Grafton, Fagg & Arbib, 1998, for details of the protocol and conditional task results).
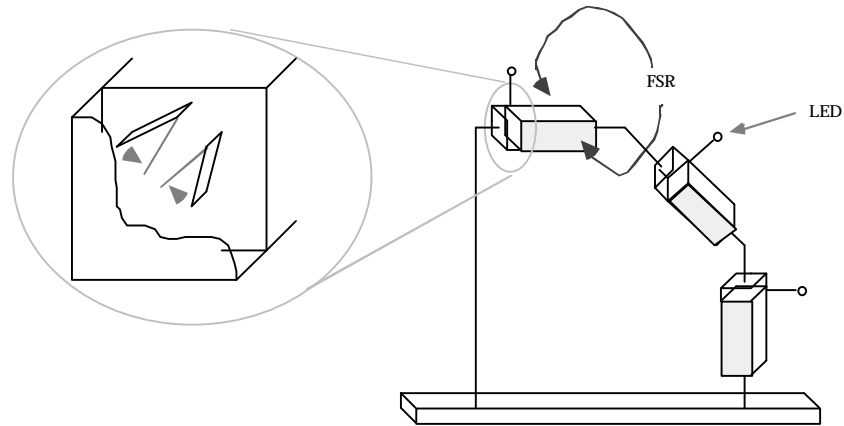
Figure 5: Apparatus used in PET experiment. Each of three stations can be grasped in two ways: precision pinch of the two plates in the grove (inset), or power grasp of the block. The side of the blocks are covered with a Force Sensitive Resistive (FSR) material; Light Emitting Diodes (LEDs), depending upon the task, indicate both the goal and type of grasp.

Subjects were asked to repeatedly perform grasping movements over the 90 second scanning period. The targets of grasping were mounted on the experimental apparatus shown in Figure 5. Each of three stations mounted on the apparatus consisted of both a rectangular block that could be grasped using a power grasp, and a pair of plates (mounted in a groove on the side of the block - see inset of Figure 5), which could be grasped using a precision pinch (thumb and index finger). A force sensitive resistive (FSR) material, mounted on the front and back of the block, detected when a solid power grasp had been established. The two plates were attached to a pair of mechanical micro-switches, which detected when a successful precision pinch had been executed. For each station, the block and plates were mounted such that the subject could grasp either one without requiring a change in wrist orientation. A bi-colored LED at each station was used to instruct the subject as to the next target of movement. A successful grasp of this next target was indicated to the subject by a change in the color of the LED. The subject then held the grasp position until the next target was given. Targets were presented every 3 +/- 0.1 seconds.

Four different scanning conditions were repeated three times each. In the first, subjects repeatedly performed a power grasp to the indicated block. The target block was identified by the turning on of the associated LED (green in color). When the subject grasped the block, the color of the LED changed from green to red. For the second condition, a precision pinch was used. The target was identified in the same manner as the first condition. In the third grasping condition (conditional task), the initial color of the LED instructed the subject to use either a precision pinch (green) or a power grasp (red). When contact was established, the LED changed to the opposite color. In the fourth (control) condition, the subjects were instructed to simply fixate on the currently lit LED, and not make movements of the arm or hand (prior to the scan, the arm was placed in a relaxed position). The lit LED changed from one position to another at the same rate and variability as in the grasping tasks. Prior to scanning, subjects were allowed to practice the tasks for several minutes.

4.1 Grasp versus Rest

Grafton, Fagg, and Arbib (1998) find that the areas most significantly active during grasping as compared with the non-movement (control) condition include sensory and motor areas along the central sulcus, as well as the nearby premotor and parietal cortices (Figure 6 left), which is consistent with a number of other similar studies with arm movements (Grafton, Fagg, Woods, & Arbib, 1996; Roland, Meyer, Shibasaki, Yamamoto, & Thompson, 1982; Winstein, Grafton, & Pohl, 1996). In addition, significant activity is observed in the inferior precentral gyrus/sulcus (indicated by the arrow in the left panel of Figure 6). This region corresponds to the ventral premotor cortex, and may include the human homologue of Rizzolatti's F5 (Winstein, et al., 1996).

4.2 Conditional versus Non-Conditional Grasp

The right panel of Figure 6 reflects differences of conditional grasp selection (power or precision based on color cues) as compared to an average of the fixed grasping conditions (power and precision tasks): Cond - (Power+Precision)/2. The upper arrow indicates a large area of significance in the left superior frontal sulcus corresponding to the dorsal premotor cortex. As earlier noted, this region in monkey is thought to be involved in the arbitrary association of stimuli with the preparation of motor programs. The lower arrow indicates increased CBF in the left inferior parietal lobule and intraparietal sulcus. Because this comparison is counterbalanced for the amount of movement made during execution of the tasks, there is no difference observed in the motor execution areas.
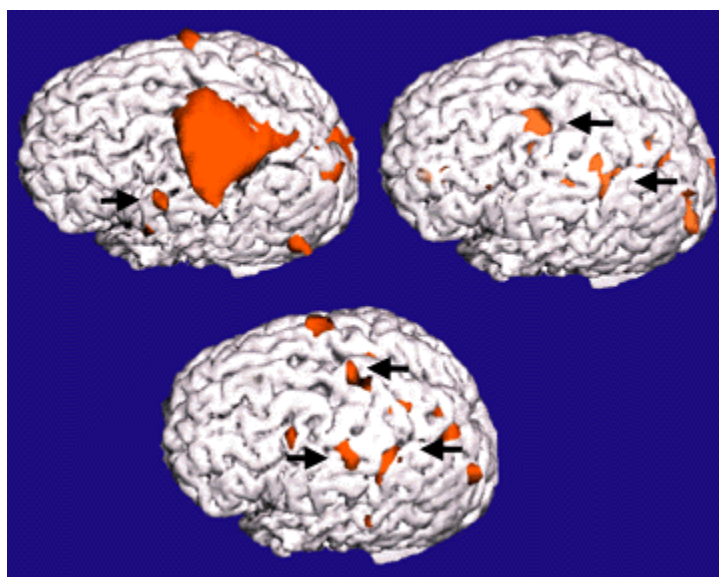

Figure 6: Left hemisphere localization of task related effects. PET statistical comparisons of the pooled data across subjects (in red, P<0.005) are superimposed on a single subject's MRI scan centered in the same coordinate space. The three panels are left superior oblique views, and denote differences of all grasp movements versus rest (left), conditional grasp selection versus fixed grasping (right), and precision versus power grasp (lower panel).

4.3 Precision versus Power Grasp

The lower panel of Figure 6 denotes areas where rCBF activity is greater for precision grasps than for power grasps. The upper arrow indicates a site located in the left dorsal frontal gyrus, in the extreme

dorsal SMA. The lower left arrow denotes a difference in the left rostral inferior parietal lobule, the lower right arrow indicates a difference in the intraparietal sulcus.

5. Comparison of PET and Synthetic PET for Grasp Control

5.1 Conditional vs. Non-Conditional Task

The model predicts that the conditional task should yield much higher activation in F2 (dorsal premotor cortex), some activation of F5, and a slight activation of AIP. The human experiment confirmed the F2 result, but failed to confirm the predictions for F5. Furthermore, in human we see an activation of the inferior parietal cortex, along the intra-parietal sulcus, which is perhaps an AIP homologue.

The negative F5 result may be used to further refine the model. Consider the functional connectivity of these regions in the model (Figure 7A). In the model, the strength of the projection from F2 to F5 is essentially a free parameter. In other words, there is a wide range of values over which the model will correctly perform the conditional and non-conditional tasks. The implication is that, by tuning this parameter, we can control this projection's contribution to the synaptic activity measure in F5. However, the difference in AIP synaptic activity from the non-conditional to the conditional task will always be less than the difference observed in F5. This results from an interaction between the neural dynamics and the assumptions made about the model anatomy. Suppose that the projection strength from F2 to F5 is increased. In this case, we would observe an increase in both F5 synaptic *and* cell activity. The increase in F5 cell activity, however, is attenuated by local, recurrent inhibitory connections. Thus the excitation that is then passed on to AIP via F5 does not reflect the full magnitude of the signal received from F2.

The conclusion is that, although we can adjust the free parameter to match one or the other observations in the human experiment (of either F5 or AIP changes), the model cannot reflect both at the same time. One possibility for repairing this problem in the model is to reroute the F2 information so that it enters the grasp decision circuitry through AIP (or both AIP and F5), rather than exclusively through F5 (Figure 7B). This would yield an increase in activity in AIP due to F2 activation with only an attenuated signal being passed on to F5, resulting in only a small increase in F5 synaptic activity. Note that we do not necessarily assume that there exists a direct cortico-cortical connection from F2 to AIP or F5, but only that there is a functional connection (which potentially involves multiple synapses).
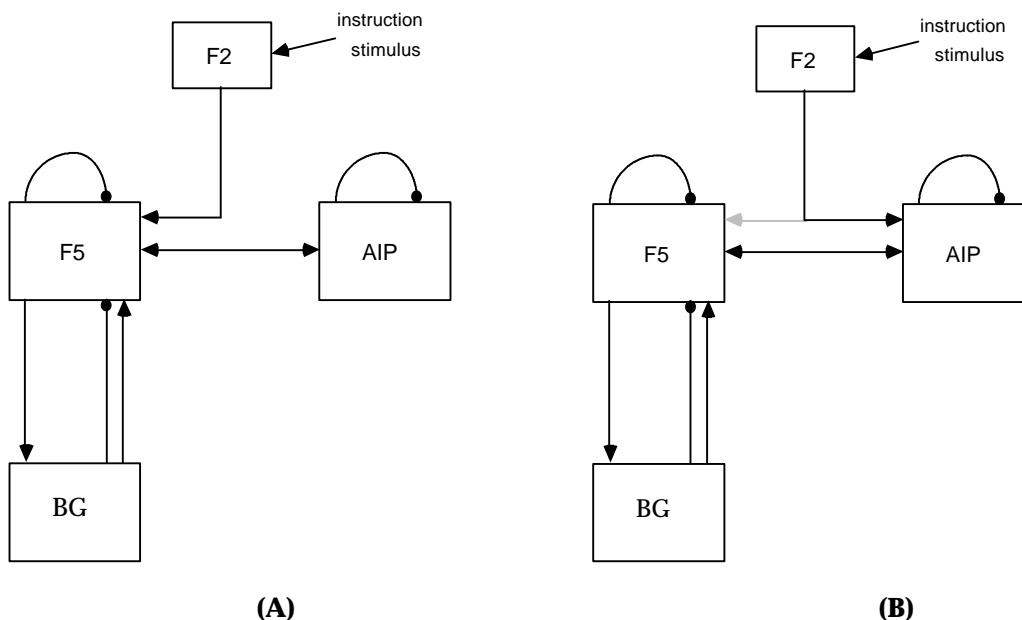
Figure 7: Previous functional model (A = Figure 2) and updated functional model (B). In the revised model, the information from F2 flows (primarily) into the circuit through a projection into AIP.

5.2 Precision vs. Power Task

The model predicts a higher degree of synaptic activity in both F5 and AIP for complex grasps than for simple grasps (in the model, these grasps are the precision pinch and power grasp, respectively). Although we see an increase in activity for the precision grasp case along the inferior parietal sulcus (IPS) in the human experiment, we fail to see any such change in the ventral premotor cortex (specifically F5). Two explanations are possible for this negative result.

First, although Rizzolatti, et al. (1988) observe a larger number of cells for the more complex grasps (e.g. the class of precision pinches), these cells may be involved in encoding the many variations of the grasp. But, when a specific grasp is executed, the number of active cells may be the same as for any other grasp instantiation (including side oppositions and power grasps). If this is the case, however, the model would also predict no difference in synaptic activity in AIP.

The second possibility assumes that the number of active F5 cells does indeed differ significantly between the precision and power grasps, but that the effect is masked by force-related activity in the region. In the human experiment, performance of the power grasp required a reasonable level of force to be applied to the block before the LED would indicate to the subject that a grasp had been detected. In monkey, force-related activity has been observed in F5 (Hepp-Reymond, Husler, Maier, & Qi, 1994). The implication is that even though there are fewer neurons involved in encoding the power grasp, they achieve a higher level of activity because of the force requirements of the task. This higher level of cell activity is an indicator of increases in the cells' inputs, which implies an increase in the rCBF measure. Thus, the rCBF measures could be similar enough in the two conditions to not be detectable above the noise levels inherent in the PET imaging process.

6. Discussion

The fundamental benefit of the Synthetic PET method is that it allows for specific predictions in PET experiments based on neural network models of behavior. Since the models themselves are a product of functional anatomy, measured single-unit recordings, and behavioral measurements, Synthetic PET provides a powerful bridge between all of these approaches. An additional strength of the Synthetic PET implementation is that the contribution of excitatory and inhibitory influences can be teased apart. Because *synaptic activity* is not the same as *neural activity*, being able to distinguish excitatory from inhibitory influences can be an aid to inferring neural activity from the rCBF measure, possibly clarifying apparent contradictions in rCBF data (an example has been demonstrated in Arbib, et al., 1995).

The low-level details of the FARS grasping model (Fagg & Arbib, 1998) were derived primarily from neurophysiological results obtained in monkey. The Synthetic PET approach extracts measures of regional synaptic activity as the model performs a variety of tasks. These measures are then compared to rCBF (regional cerebral blood flow) observed during human PET experiments as the subjects perform tasks similar to those simulated in the model. In some cases, the human results provide confirmation of the model behavior. In other cases, where there is a mismatch between model prediction and human results, it is possible (as we have shown) to use these negative results to further refine and constrain the model and, on this basis, design new experiments for both primate neurophysiology and human brain imaging.

An additional feature of the Synthetic PET technique is that it provides a link between neural network models and anatomic circuitry with the results displayed directly on a brain atlas centered in Talairach coordinates (Talairach & Tournoux, 1988). This facilitates interaction between anatomists, physiologists and modelers interested in common neurobehavioral phenomena. The method is sufficiently flexible that it will be possible to have network implementations spanning multiple species. Homologies and differences between species can then be tested more rigorously using predictions generated by the Synthetic PET , while the human data provide another form of validation of neural network models derived from monkey data.

Our current measure of "raw PET activity", based on a linear function of the total of the absolute value of synaptic activity, already yields *qualitatively* useful results in evaluating the sign and small versus large magnitude of activities seen in PET comparisons. However, we do not claim that this first approximation yields *quantitatively* accurate predictions. We note, as a target for further research on Synthetic brain imaging, the interest of evaluating a variety of more quantitative fits based on (possibly nonlinear) combinations of cell firing rates, synaptic change, and synaptic activity per se. We also note the possibility of performing a stochastic analysis with the model in order to account for the variation in PET activity seen in the same subject over a set of trials.

7. Acknowledgments

8. References

Arbib, M. A. (1995c). Part I: The Background. In M. A. Arbib (Eds.), The Handbook of Brain Theory and Neural Networks (pp. 3-25). A Bradford Book/The MIT Press.

Arbib, M.A., Billard, A., Iacoboni, M., and Oztop, E. (2000). Synthetic Brain Imaging: Grasping, Mirror Neurons and Imitation, *Neural Networks*, **13**, 975-997.

Arbib, M. A., Bischoff, A., Fagg, A. H., & Grafton, S. T. (1995). Synthetic PET: Analyzing Large-Scale Properties of Neural Networks. *Human Brain Mapping*, **2**, 225-33.

Binkofski, F., Amunts, K., Stephan, K. M., Posse, S., Schormann, T., Freund, H.-J., Zilles, K., & Seitz, J. (2000). Broca's Region Subserves Imagery of Motion: A Combined Cytoarchitectonic and fMRI Study. *Human Brain Mapping*, **11**, 273-85.

Binkofski, F., Buccino, G., Posse, S., Seitz, R. J., Rizzolatti, G., & Freund, H.-J. (1999). A Fronto-Parietal Circuit for Object Manipulation in Man: Evidence from an fMRI-study. *European Journal of Neuroscience*, **11**, 3276-86.

Bota, M., and Arbib, M.A., 2001, The Neurohomology Database, in *Computing the Brain: A Guide to Neuroinformatics*, (M.A. Arbib, and J.S. Grethe, Eds.), San Diego: Academic Press, pp.337-351.

Brownell, G. L., Budinger, T. F., Lauterbur, P. C., & McGeer, P. L. (1982). Positron Tomography and Nuclear Magnetic Resonance Imaging. *Science*, **215**, 619-26.

Buccino, G., Binkofski, F., Fink, G. R., Fadiga, L., Fogassi, L., Gallese, V., Seitz, R. J., Zilles, K., Rizzolatti, G., & Freund, H.-J. (2001). Action Observation Activates Premotor and Parietal Areas in a Somatotopic Manner: an fMRI Study. *European Journal of Neuroscience*, **13**, 400-4.

Ehrsson, H. H., Fabergren, A., Jonsson, T., Westling, G., Johansson, R. S., & Forssberg, H. (2000). Cortical Activity in Precision- Versus Power-Grip Tasks: An fMRI Study, *Journal of Neurophysiology*, **83**(1), 528-36.

Evarts, E. V., Shinoda, Y., & Wise, S. P. (1984). *Neurophysiological Approaches to Higher Brain Function*. New York: Wiley-Interscience Press.

Fagg, A. H. (1996) *A Computational Model of the Cortical Mechanisms Involved in Primate Grasping*. PhD Dissertation, University of Southern California, Computer Science Deptartment. Available at: http://www-robotics.usc.edu /~af0a/thesis/.

Fagg, A. H., & Arbib, M. A. (1992). A Model of Primate Visual-Motor Conditional Learning. *Journal of Adaptive Behavior*, **1**(1), 3-37.

Fagg, A. H., & Arbib, M. A. (1998). Modeling Parietal-Premotor Interactions in Primate Control of Grasping. *Neural Networks*, **11**(7/8), 1277-1303.

Fox, P. T., & Raichle, M. E. (1985). Stimulus Rate Determines Regional Brain Flow In Striate Cortex. *Annals of Neurology*, **17**, 303-5.

Grafton, S. T., Fagg, A. H., & Arbib, M. A. (1998). Dorsal Premotor Cortex and Conditional Movement Selection: A PET Functional Mapping Study. *Journal of Neurophysiology*, **79**(2), 1092-7.

Grafton, S. T., Fagg, A. H., Woods, R. P., & Arbib, M. A. (1996). Functional Anatomy of Pointing and Grasping in Humans. *Cerebral Cortex*, **6**(2), 226-37.

Hepp-Reymond, M. C., Husler, E. J., Maier, M. A., & Qi, H. X. (1994). Force-Related Neuronal-Activity in 2 Regions of the Primate Ventral Premotor Cortex. *Canadian Journal of Physiology and Pharmacology*, **72**(5), 571-9.

Kinoshita, H., Oku, N., Hashikawa, K., & Nishimura, T. (2000). Functional Brain Areas Used for the Lifting of Objects Using a Precision Grip: a PET study. *Brain Research*, **857**, 119-30.

Kurata, K., & Wise, S. P. (1988). Premotor Cortex of Rhesus Monkeys: Set-Related Activity During Two Conditional Motor Tasks. *Experimental Brain Research*, **69**(2), 327-43.

Kurata, K., Tsuji, T., Naraki, S., Seino, M., & Abe, Y. (2000). Activation of the Dorsal Premotor Cortex and Pre-Supplementary Motor Area of Humans During an Auditory Conditional Motor Task, *Journal of Neurophysiology*, **84**(3), 1667-72.

Mitz, A. R., Godshalk, M., & Wise, S. P. (1991). Learning-Dependent Neuronal Activity in the Premotor Cortex. *Journal of Neuroscience*, **11**(6), 1855-72.

Rall, W. (1995). Perspective on Neuron Model Complexity. In M. A. Arbib (Eds.), The Handbook of Brain Theory and Neural Networks (pp. 728-732). A Bradford Book/The MIT Press.

Rizzolatti, G., Camarda, R., Fogassi, L., Gentilucci, M., Luppino, G., & Matelli, M. (1988). Functional Organization of Inferior Area 6 in the Macaque Monkey II. Area F5 and the Control of Distal Movements. *Experimental Brain Research*, **71**, 491-507.

Roland, P. E., Meyer, E., Shibasaki, T., Yamamoto, Y. L., & Thompson, C. J. (1982). Regional cerebral blood flow changes in cortex and basal ganglia during voluntary movements in normal human volunteers. *Journal of Neurophysiology*, **48**, 467-80.

Taira, M., Mine, S., Georgopoulos, A. P., Murata, A., & Sakata, H. (1990). Parietal Cortex Neurons of the Monkey Related to the Visual Guidance of Hand Movement. *Experimental Brain Research*, **83**, 29-36.

Talairach, J., & Tournoux, P. (1988). *Co-planar Stereotaxic Atlas of the Brain*. New York: Thieme Medical Publishers.

Tanji, J., & Keisetsu, S. (1994). Role for Supplementary Motor Area Cells in Planning Several Movements Ahead. *Nature*, **371**(29), 413-6.

Winstein, C. J., Grafton, S. T., & Pohl, P. S. (1996). Motor task difficulty and brain activity: an investigation of goal-directed reciprocal aiming using positron emission tomography (PET). *Journal of Neurophysiology*, **77**, 1581-94.

Wise, S. P., & Mauritz, K. H. (1985). Set-related Neuronal Activity in the Premotor Cortex of Rhesus Monkeys: Effects of Changes in Motor Set. In *Proceedings of the Royal Society of London*, **223** (pp. 331-54).